



Variations of Mediterranean–Atlantic exchange across the late Pliocene climate transition

Ángela García-Gallardo¹, Patrick Grunert¹, Werner E. Piller¹

5 ¹Institute of Earth Sciences, University of Graz, NAWI Graz Geocenter, Heinrichstrasse 26, 8010 Graz, Austria.

Correspondence to: Ángela García-Gallardo (angela.garcia-gallardo@uni-graz.at)

Abstract. Mediterranean-Atlantic exchange through the Strait of Gibraltar plays a significant role in the
10 global ocean-climate dynamics in two ways. On one side, the injection of the saline and warm Mediterranean Outflow Water (MOW) contributes to North Atlantic deep-water formation. In return, the Atlantic inflow is considered a sink of less saline water for the North Atlantic Ocean. However, while the history of MOW is the focus of numerous studies, the latter has received little attention so far. The present study provides an assessment of the Mediterranean–Atlantic exchange with focus on the
15 Atlantic inflow strength and its response to regional and global climate from 3.33 to 2.60 Myrs. This time interval comprises the mid-Pliocene warm period (MPWP, 3.29–2.97 Myr) and the onset of the Northern Hemisphere Glaciation (NHG). For this purpose, gradients in surface $\delta^{18}\text{O}$ records of the planktonic foraminifer *Globigerinoides ruber* between the Integrated Ocean Drilling Program (IODP) Hole U1389E (Gulf of Cadiz) and ODP Site 978 (Alboran Sea) have been evaluated. Interglacial stages and warm glacial
20 of the MPWP revealed steep and reversed (relative to the present) W-E $\delta^{18}\text{O}$ gradients suggesting a weakening of Mediterranean–Atlantic exchange likely caused by high levels of relative humidity in the Mediterranean region. In contrast, periods of stronger inflow are indicated by flat $\delta^{18}\text{O}$ gradients due to more intense arid conditions during the severe glacial Marine Isotope Stage (MIS) M2 and the initiation of the NHG (MIS G22, G14, G6–104). Intensified Mediterranean–Atlantic exchange in cold periods is
25 linked to the occurrence of ice-rafted debris (IRD) at low latitudes and weakening of the Atlantic Meridional Overturning Circulation (AMOC). Our results thus suggest the development of a negative feedback between AMOC and exchange rates at the Strait of Gibraltar in the latest Pliocene as it has been proposed for the late Quaternary.



Keywords. Atlantic inflow; Mediterranean Outflow Water; *Globigerinoides ruber*; oxygen isotopes; Mid-
30 Pliocene Warm Period; Northern Hemisphere Glaciation.

1 Introduction

Mediterranean–Atlantic water mass exchange through the Strait of Gibraltar is driven by a two
directional current system in which the westward outflow of warm and saline Mediterranean Outflow
35 Water (MOW) at the bottom, driven by excess evaporation in the Mediterranean, is compensated by the
inflow of colder and less saline North Atlantic Central Water (NACW) at the surface (Bormans et al.,
1986; Ochoa and Bray, 1991; Vargas-Yáñez et al., 2002). **Mediterranean–Atlantic exchange** plays an
important role for regional and global climate in two respects. First, the injection of warm and salty
MOW into the North Atlantic contributes to deep water formation at high latitudes, and thus to the
40 dynamics of the ocean–climate system (Bryden and Kinder, 1991; Ivanovic et al., 2014; Reid, 1979;
Rogerson et al., 2012; Voelker et al., 2006). Second, the eastward Atlantic inflow has been considered a
freshwater sink for the North Atlantic since less saline North Atlantic Central Water is replaced with
saltier MOW (Rogerson et al., 2010). **As a result of this interaction, a negative feedback between
exchange and Atlantic Meridional Overturning Circulation (AMOC) has been recognized during Heinrich
45 Stadials in the late Quaternary** (Rogerson et al., 2010, 2012).

Previous research has focused strongly on MOW variability since the Pliocene (e.g. Bryden and Stommel,
1982; Hernández-Molina et al., 2014; Iorga and Lozier, 1999; Kaboth et al., 2016; Voelker et al., 2006)
but has neglected the Atlantic surface water component (Rogerson et al., 2010). Furthermore, there are
a number of studies on Mediterranean–Atlantic exchange during the early-mid Pliocene and early
50 Pleistocene (e.g., **Bahr et al., 2015**; García-Gallardo et al., 2017; Grunert et al., 2017; Hernández-Molina
et al., 2014; Kaboth et al., 2017; Khélifi et al. 2009, 2014; Van der Schee et al., 2016; Voelker et al., 2015)
leaving a gap in our knowledge about the late Pliocene climate transition comprising the mid-Pliocene
warm period (MPWP) and the initiation of the Northern Hemisphere Glaciation (NHG).

The MPWP (3.29–2.97 Myr) has been identified by the United States Geological Survey’s PRISM (Pliocene
55 Research, Interpretation and Synoptic Mapping; Haywood et al., 2010) group as a potential analogue for
the future of global climate due to remarkable similarities with model predictions (Dowsett et al., 2012;



Robinson et al., 2008). These include increased levels of greenhouse gases up to 350–450 ppmv, global temperatures increased by 1–5 °C relative to today, and increased annual precipitation and elevated sea level (Budyko et al., 1985; Fauquette et al., 1998; Haywood and Valdes, 2004; Lunt et al., 2012; Pagani et al., 2010; Raymo et al., 1996; Seki et al., 2010). At ~3.3 Ma, a severe ice sheet expansion initiated glacial Marine Isotopic Stage (MIS) M2, a precursor for the initiation of NHG at 2.95 Ma (Bartoli et al., 2006).
60 **The strong glacial conditions of MIS M2 have been considered a trigger of long-term intensification of Mediterranean–Atlantic exchange** (Khélifi et al., 2014; Sarnthein et al., 2017).

The present study aims for the reconstruction of variations in Mediterranean–Atlantic exchange with strong focus on the Atlantic inflow throughout the MPWP and the onset of the NHG. The Integrated Ocean Drilling Program (IODP) Hole U1389E has been used as the reference location for the Gulf of Cadiz and Ocean Drilling Program (ODP) Site 978 for the Alboran Sea. Planktonic $\delta^{18}\text{O}$ records obtained from both sites were used for the reconstruction of isotopic gradients as indicators of Atlantic inflow strength across the late Pliocene climate transition.

70

2 Regional setting

2.1 Alboran Sea – ODP Site 978

ODP Site 978 is located in the Alboran Sea north of the Al-Mansour Seamount (36°13'N, 02°03'W; Fig. 1) at 1930 m water depth (Comas et al., 1996). Circulation in the Alboran Sea is driven by three water mass layers. At the surface (0 – ~200 m), inflowing Atlantic water enters the Mediterranean basin (Millot, 1999). On its way, it mixes with upwelled MOW within the Strait of Gibraltar (Folkard et al., 1997) and with surface waters of the Alboran Sea, creating the Modified Atlantic Water with temperatures of 15–16 °C and salinity of 36.5 (Millot, 1999), which follows two anticyclonic gyres, the Western Alboran Gyre (WAG) and the Eastern Alboran Gyre (EAG) (Gascard and Richez, 1985; Vargas-Yáñez et al., 2002). The northern Alboran Sea is affected by upwelling along the Spanish coast providing nutrients and enhanced primary productivity (Minas et al., 1991; Peeters et al., 2002; Sarhan et al., 2000). The bottom layer is represented by the Western Mediterranean Deep water (WMDW; water temperature ~ 13 °C, salinity ~ 38.5) below 1000 m, formed due to overturning in the Gulf of Lions (Bryden et al., 1994; Hernández-Molina et al., 2006; Millot, 1999; Rhein, 1995). The intermediate layer found between ~ 200 and 1000 m
80



85 is composed of the salty (up to 39.1) and warm (14.7 to 17 °C) Levantine Intermediate water (LIW) which originates from overturning in the Eastern Mediterranean (Millot, 2013; Wüst, 1961). Finally, WMDW, together with LIW, exit the Mediterranean basin through the Strait of Gibraltar and form MOW in the Gulf of Cadiz (Bryden et al., 1994).

2.2 Gulf of Cadiz – IODP Hole U1389E

90 IODP Hole U1389E is located in the northern Gulf of Cadiz (36°25.515'N, 07°16.683'W; Fig. 1) at 644 m water depth under direct influence of MOW. It constitutes a key site for the recovery of an upper Pliocene contourite succession (Stow et al., 2013). Once LIW and WMDW exit the Strait of Gibraltar and form MOW, this water mass splits into two plumes due to the complex morphology of the continental slope in the Gulf of Cadiz. The upper plume flows between 500 and 800 m while the lower plume flows
95 between 800 and 1400 m (Ambar and Howe, 1979; Borenäs et al., 2002; García et al., 2009; Llave et al., 2007; Madelain, 1970; Marchès et al., 2007; Serra et al., 2005; Zenk, 1975). Surface circulation in the Gulf of Cadiz is governed by the Gulf of Cadiz slope current, flowing eastward along the western Iberian margin and the offshore inflow which meet at the Strait of Gibraltar and enter the Mediterranean basin (Peliz et al., 2009).

100

3 Material and methods

3.1 Sample material and data collection

This study relies on published and newly acquired stable oxygen isotope ($\delta^{18}\text{O}$) records of the planktonic foraminifer *Globigerinoides ruber* from upper Pliocene (3.33–2.60 Myrs) sediments at Site 978 (Alboran
105 Sea), Hole U1389E (Gulf of Cadiz) and the Rossello section in Sicily (Fig. 1). Sediment cores from ODP Site 978 were recovered during ODP Leg 161 (Comas et al., 1996). Khélifi et al. (2014) have established a $\delta^{18}\text{O}$ record from *Gdes. ruber* for this site which ranges from 3.60 to 2.70 Myrs (cores 26R–20R, 438.38–371.00 mbsf). For the purpose of our study, this record was extended to 2.60 Ma through analyses of new samples collected every 50 cm from core sections 19R-5 through 16R-4 at the Bremen Core
110 Repository.



Sediment cores from Hole U1389E were obtained during IODP Expedition 339 (Stow et al., 2013). A $\delta^{18}\text{O}$ record of *Gdes. ruber* ranging from 3.70 to 2.60 Myrs (cores 70R–41R, 982.78–703.62 mbsf) has been established by Grunert et al. (2017) and adopted for this study.

The stacked $\delta^{18}\text{O}$ record of Lourens et al. (1992, 1996) from the Rossello outcrops in Sicily has been
115 adopted for stratigraphic calibration of the new $\delta^{18}\text{O}$ record at Site 978.

3.2 Stable isotope analysis

Details on laboratory protocols and isotopic analyses performed by Grunert et al. (2017), Khélifi et al. (2014) and Lourens et al. (1996) can be found in the respective publications. For the continuation of the Site 978 record, samples from core sections 19R-5 to 16R-4 were analyzed every 50 cm. Sediment
120 samples were dried, weighed, washed through sieves 250 and 63 μm and dried. Whenever possible, 10 to 20 well-preserved specimens of *Gdes. ruber* $> 250 \mu\text{m}$ were picked for isotopic analysis. Crushed and cleaned shells were reacted with 100% phosphoric acid at 70 °C using a Gasbench II connected to a ThermoFisher Delta V Plus mass spectrometer at GeoZentrum Nordbayern (Erlangen). All values are reported in per mil relative to VPDB. Reproducibility and accuracy were monitored by replicate analysis
125 of laboratory standards calibrated by assigning $\delta^{13}\text{C}$ values of +1.95‰ to NBS19 and -46.6‰ to LSVEC and $\delta^{18}\text{O}$ values of -2.20‰ to NBS19 and -23.2‰ to NBS18.

3.3 Age model

Age constraints for Site 978 are established from 3.6 to 2.8 Myrs by Khélifi et al. (2014) and those for Hole U1389E are reported in Grunert et al. (2017). The latter study establishes the correlation of the $\delta^{18}\text{O}$
130 record of Hole U1389E to Site 978 from Khélifi et al. (2014). However, in the upper part ($< 2.75 \text{ Ma}$), Hole U1389E is correlated to the Rossello section because the Site 978 record ends there. To ensure comparability, the newer $\delta^{18}\text{O}$ record obtained in this study for Site 978 has been visually correlated to the Rossello section and includes the biostratigraphic event at 2.72 Ma with the first occurrence of the planktonic foraminifer *Neoglobobadrina atlantica* (Fig. 2-a; Lourens et al., 1996). Identification and
135 denomination of Marine Isotopic Stages (MIS) has been established according to Lourens et al. (1996; Figs. 3, 4-a).



3.4 Glacial–interglacial $\delta^{18}\text{O}$ gradients across the Strait of Gibraltar

A compilation of the late Pliocene (3.33–2.60 Myrs) $\delta^{18}\text{O}$ records from the two studied sites are shown in Fig. 3 (Supplementary Table 1). Based on the average $\delta^{18}\text{O}$ values of glacial–interglacial MIS (see Supplementary Table 2), gradients between the corresponding stages in the Gulf of Cadiz (Hole U1389E) and the Alboran Sea (Site 978) have been established (Fig. 4-b) by a regression line that represents the slope of $\delta^{18}\text{O}$ per degree of longitude.

4 Results

4.1 Age model for the new $\delta^{18}\text{O}$ record of ODP Site 978 (369–337 mbsf)

The new $\delta^{18}\text{O}$ record from the upper part of Site 978 is visually correlated to the Rossello section relying on established biostratigraphic tie points (Fig. 2-a; Gradstein et al., 2012). The last occurrences of *Discoaster tamalis* (2.80 Ma), *D. surculus* (2.49 Ma) and *D. pentaradiatus* (2.39 Ma) have been documented in Comas et al. (1996). In addition, the first occurrence of *Neogloboquadrina atlantica* (sin) is here recorded in core section 19R-6 at 362.78 mbsf suggesting an age of ~ 2.72 Ma (Lourens et al., 1996). Our age model for OPD Site 978 indicates that the Pliocene/Pleistocene boundary at ~ 2.59 Ma is located at ~ 340 mbsf (Fig. 2-a). Sedimentation rates calculated for this interval vary from 0.06 to 0.57 m/ka (mean: 0.26 m/ka; Fig. 2-b).

4.2 Glacial/interglacial $\delta^{18}\text{O}$ gradients

$\delta^{18}\text{O}$ values for intervals I to III are shown vs. longitude in Fig. 3. Hole U1389E suffers from notable gaps throughout the studied interval due to poor core recovery (Fig., 3; Stow et al., 2013; Grunert et al., 2017). For this reason, the section is subdivided into three well recovered intervals with continuous $\delta^{18}\text{O}$ records which will be in the focus of our study (Interval I: 3.33–3.27 Myrs; Interval II: 3.02–2.88 Myrs; Interval III: 2.73–2.60 Myrs; Figs. 3, 4-a).

In Interval I (3.33–3.27 Myrs), mean $\delta^{18}\text{O}$ values of Hole U1389E (Min: - 1.22 ‰; Max: + 0.46 ‰; Mean: - 0.34 ‰) and Site 978 (Min: - 1.34 ‰; Max: + 0.49 ‰; Mean: - 0.39 ‰) are close to each other (Fig. 4-a1; Table 1). $\delta^{18}\text{O}$ gradients between Site 978 and Hole U1389E change direction from interglacial MIS MG1 to glacial MIS M2 (Figs. 4-a1, 4-b1). $\delta^{18}\text{O}$ data from interglacial MIS MG1 reveals higher values in the Gulf



of Cadiz compared to the Alboran Sea resulting in an isotopic gradient of $-0.08 \text{ ‰ degree}^{-1}$. In contrast,
165 glacial period MIS M2 shows an opposite isotopic gradient ranging from $+0.05$ to $+0.09 \text{ ‰ degree}^{-1}$ for
the two intermittent $\delta^{18}\text{O}$ maxima M2.1 and M2.2, respectively (Fig. 4-b1).

In Interval II (3.02–2.88 Myrs), mean $\delta^{18}\text{O}$ values of Hole U1389E (Min: -0.99 ‰ ; Max: $+0.98 \text{ ‰}$; Mean: -0.16 ‰) are considerably lighter compared to Site 978 (Min: -1.64 ‰ ; Max: $+0.50 \text{ ‰}$; Mean: -0.50 ‰)
(Fig., 4-a2; Table 1). The records are particularly well separated during $\delta^{18}\text{O}$ minima whereas they
170 converge during maxima (Fig. 4-a2). Interglacial periods MIS G21, G19 and G15 and glacial periods MIS
G22, G20 and G16 show isotopic gradients ranging from -0.06 to $-0.13 \text{ ‰ degree}^{-1}$ and -0.04 to -0.12
 ‰ degree^{-1} , respectively (Fig. 4-b2). The only exception occurs during glacial period MIS G14 which
shows a positive and relatively flat gradient of $+0.03 \text{ ‰ degree}^{-1}$.

In Interval III (2.73–2.60 Myrs), mean $\delta^{18}\text{O}$ values are again closer to each other (Hole U1389E: Min: -0.85 ‰ ;
175 Max: $+0.70 \text{ ‰}$; Mean: -0.05 ‰ and Site 978: Min: -1.11 ‰ ; Max: $+0.54 \text{ ‰}$; Mean: -0.20 ‰)
(Fig. 4-a3, Table 1). A wide range of $\delta^{18}\text{O}$ gradients has been calculated for Interval III (Fig. 4-b3).
Interglacial periods MIS G7, G5 and G3 as well as glacial period MIS G4 show negative $\delta^{18}\text{O}$ gradients
between -0.03 and $-0.10 \text{ ‰ degree}^{-1}$. In contrast, glacial periods MIS G6, G2 and 104 reveal positive
 $\delta^{18}\text{O}$ gradients ranging from $+0.02$ to $+0.06 \text{ ‰ degree}^{-1}$ (Fig. 4-b3).

180

5 Discussion

5.1 Direction of $\delta^{18}\text{O}$ gradients

Our late Pliocene data set is based on the planktonic *Gdes. ruber*, yet recent $\delta^{18}\text{O}$ gradients between the
Gulf of Cadiz and the Alboran Sea have been established from the planktonic *Globigerina bulloides* (e.g.
185 Cacho et al., 2001; Rogerson et al., 2010). A seasonal $\delta^{18}\text{O}$ offset between *Gdes. ruber* (blooming in
spring-summer) and *G. bulloides* (fall-winter) is evident from core top and parallel down core records of
 $\delta^{18}\text{O}$ in the late Quaternary (Figs. 5-a, 5-b; Voelker et al., 2009). However, despite this offset, the $\delta^{18}\text{O}$
gradients obtained from both species (*G. bulloides*: Rogerson et al., 2010; *Gdes. ruber*: Rohling, 1999 and
Salgueiro et al., 2008) show the same gradient direction with lighter $\delta^{18}\text{O}$ values in the Gulf of Cadiz and
190 heavier values in the Alboran Sea (Fig. 5-b). Previous studies further show that the direction of this W-E
gradient has not changed over the last $\sim 25,000$ years (Cacho et al., 2001; Rogerson et al., 2010). For the



late Pliocene, however, our data suggest that the $\delta^{18}\text{O}$ gradient was considerably more variable, particularly during glacial stages (Figs. 4-a, 4-b). While all studied interglacial stages and glacial stages G22–G16 (except G14) of Interval II show a reversed gradient with respect to the present, the strong
195 glaci-als M2, G14, G6, G2 and 104 show a gradient in line with present-day observations (Figs. 4-b, 5b).

Seasonal variations of Atlantic inflow reported in previous studies (e.g. Bormans et al., 1986; Ovcchinnikov, 1974; Parada and Cantón, 1998; Vargas-Yáñez et al., 2002) can be the cause of Sea Surface Salinity (SSS) and Sea Surface Temperature (SST) variability. While seasonal changes of SSS are < 0.5 , SST variability is more prominent and may result in brief temporary reversals of SST gradients (MEDATLAS,
200 2002; Rogerson et al., 2010). The Alboran Sea shows colder temperatures than the Gulf of Cadiz during all seasons due to upwelling, with occasional exceptions in summer under the influence of easterly winds (Bakun and Agostini, 2001; Folkard et al., 1997; Peeters et al., 2002; Rogerson et al., 2010; Sarhan et al., 2000; Shaltout and Omstedt, 2014). The $\delta^{18}\text{O}$ composition of present-day seawater is thus considered to be largely determined by changes of SST (Rogerson et al., 2010).

205 Reversed gradients in the late Pliocene could imply a different SST gradient due to a different current regime and/or lack of upwelling in the Alboran Sea in the Pliocene. Unfortunately, there is little data on SST available from the late Pliocene which would allow further evaluation. Khélifi et al. (2014) provide an alkenone-based SST record from Site 978 from ~ 3.6 to 2.7 Myrs (Intervals I and II of this study) which indicates SSTs ranging from ~ 26.5 to 27.5 °C. A comparable alkenone-based SST reconstruction is
210 available from IODP Site U1387 in the Gulf of Cadiz and suggests an SST-range from ~ 26 to 27 °C from ~ 6 to 2.7 Myrs (Tzanova and Herbert, 2015). The comparison thus suggests that the difference in SST between the two sites was little to none, with surface waters in the Gulf of Cadiz probably slightly colder than in the Alboran Sea. Given a temperature sensitivity of ~ 0.23 ‰ °C⁻¹ for planktonic foraminifera (O'Neill et al., 1969), estimated SST offsets cannot fully explain $\delta^{18}\text{O}$ gradients < -0.05 ‰ degree⁻¹ in our
215 case.

Variations of $\delta^{18}\text{O}$ gradients between the Mediterranean and Atlantic have also been explored in modeling studies by Rohling (1999). This model indicates that the direction of the gradient is largely influenced by relative humidity in the Mediterranean. While relative humidity values similar to present-day (which also persisted during the LGM; Rohling, 1999; cf. Rogerson et al., 2010) recreate $\delta^{18}\text{O}$
220 gradients as observed in Holocene and late Pleistocene foraminiferal records accurately, an increase of 5% in relative humidity is sufficient to reverse the $\delta^{18}\text{O}$ gradient due to isotopic depletion in the



Mediterranean (Rohling, 1999). Pollen-based data suggest that annual precipitation and humidity in the Mediterranean were considerably higher relative to present-day levels during most of the late Pliocene with the exception of the strong glacial periods M2, G22, and G6–104 (Bertini, 2010; Fauquette et al., 1998). A warmer and more humid climate implies higher runoff and freshening of the Mediterranean surface waters leading to depleted $\delta^{18}\text{O}$ records as reported from Pliocene to Holocene in previous studies (e.g. Gudjonsson and van der Zwaan, 1985; Kaboth et al., 2017; Thunell and Williams, 1989; Van Os et al., 1994; Vergnaud-Grazzini et al., 1977). We thus consider $\delta^{18}\text{O}$ depletion of Mediterranean waters during a warm and humid paleoclimate as the most likely explanation for the reversed gradients observed for interglacial stages from all three studied intervals as well as for the comparably warm glacial periods MIS G22, G20, G16, and G4 (Fig. 4-b). Conversely, arid conditions are indicated by pollen data only for the strong glacial stages M2, G6, G2, and 104 which herald increasing Northern Hemisphere Glaciation and for which our data suggest $\delta^{18}\text{O}$ gradients similar to the present (Fauquette et al., 1998; Figs. 4-b, 5-b).

235 5.2 Steepness of $\delta^{18}\text{O}$ gradients

While **humidity likely explains large-scale variations** of normal and reversed $\delta^{18}\text{O}$ gradients in the late Pliocene relative to the present-day trend, slope steepness is considered sensitive to regional signals, i.e. it responds to the strength of surface water exchange across the Strait of Gibraltar (Rohling, 1999; Rogerson et al., 2010). **Whereas** flat gradients are indicative of well-connected basins and enhanced exchange, steeper gradients suggest more restricted conditions and reduced exchange (Rogerson et al., 2010).

The steepness of present-day gradients varies from 0.05 to 0.13 ‰ degree⁻¹ depending on the time of calcification of *Gdes. ruber* and *G. bulloides* (Fig. 5-b; this study; Rogerson et al., 2010; see chapter 5.1). In addition, Rogerson et al. (2010) reported a gradient of 0.26 ‰ degree⁻¹ during the Last Glacial Maximum and of 0.01 and 0.14 ‰ degree⁻¹ during Heinrich Stadials 1 and 2, respectively. Regardless of the direction, the steepness of late Pliocene slopes ranges from 0.05 to 0.13 ‰ degree⁻¹ in all interglacial stages (except MIS G5) and glacial stages M2, G20, G16, and 104 (Fig. 4-b), thus indicating exchange rates which are similar or reduced to present-day values. In contrast, flatter gradients during glacial stages MIS G22, G14, G6, and G2 (0.02 to 0.04 ‰ degree⁻¹; Figs. 4-b2, 4-b3) point to enhanced exchange during these cold periods.



Support for our interpretation comes from available studies on MOW development during the late Pliocene to which the strength of AMOC is directly linked. The onset of long-term intensification of MOW has been linked to arid conditions during glacial stage M2, a second pulse occurs at ~ 2.8-2.7 (Grunert et al., 2017; Hernández-Molina et al., 2014; Khélifi et al., 2009; 2014; Sarnthein et al., 2017). Both pulses occur during these glacial periods in which we observe gradients similar to today and their succession is reflected in a flattening of gradients with the onset of NHG. Fluctuations of MOW intensity in the late Pliocene is in turn linked to global climate processes. Kleiven et al. (2002) demonstrated that lowered values of benthic $\delta^{13}\text{C}$ in the North Atlantic during glacial stages (MIS M2, G22, G16, G6–104 of our study) were related to a decreased production of North Atlantic Deep Water (NADW; Fig. 4-a) at high latitudes. Furthermore, periods of reduced Atlantic Meridional Overturning Circulation are linked to freshening of surface waters in the North Atlantic due to the increased iceberg melting and influx of ice-rafted debris (IRD) (Kleiven et al., 2002). Despite a strong influx of IRD occurs at northern latitudes during MIS M2, the first occurrence of IRD at low mid-latitudes is recorded during G14 in samples from Deep Sea Drilling Program (DSDP) Site 607 with following peaks during glacials G6–104 (Bailey et al., 2010; Kleiven et al., 2002; Fig. 4-a). Thus, enhanced Mediterranean–Atlantic exchange suggested for MIS M2 parallels a drop of NADW production and weakened AMOC (DeSchepper et al., 2009; Khélifi et al., 2014; Sarnthein et al., 2017). Continuous occurrences of IRD at low mid-latitudes and reduced AMOC during glacial periods G14 to 104 fall together with intensified Mediterranean–Atlantic exchange during strong glacial periods at the onset of the NHG. In contrast, the lack of IRD and increased $\delta^{13}\text{C}$ observed during interglacials (Kleiven et al., 2002) is in accordance with more restricted exchange during MIS MG1, G21, G19, G15, G5, and G3 (Fig. 4-a). The observed negative feedback between AMOC and Mediterranean–Atlantic exchange at the onset of the NHG seems to work similarly as during Heinrich Stadials from the Holocene as reported by Rogerson et al. (2010). However, higher resolution of our Pliocene records would be necessary to establish an accurate assessment of the timing of these feedback mechanisms within the glacial periods.

6 Conclusions

Late Pliocene $\delta^{18}\text{O}$ gradients of the planktonic foraminifer *Globigerinoides ruber* from IODP Hole U1389E (Gulf of Cadiz) and ODP Site 978 (Alboran Sea) allowed the reconstruction of Mediterranean–Atlantic exchange variations between 3.33 and 2.60 Myrs, spanning the transition from the MPWP into the NHG.



The $\delta^{18}\text{O}$ gradients across the Strait of Gibraltar have been analyzed for individual glacial and interglacial stages in terms of direction and steepness.

In contrast to positive gradients in the present-day, elevated levels of humidity during the MPWP caused reversed and steep $\delta^{18}\text{O}$ gradients in the late Pliocene, especially during interglacial stages. Increased
285 aridity caused a shift to positive gradients during strong glacial periods at MIS M2 and the onset of the NHG (MIS G22, G14, G2–104). **Flat slopes indicate enhanced inflow during those cold periods.**

Intensified MOW has been reported during M2 and from 2.8 Ma coinciding with intense glacial stages. Strengthened Mediterranean–Atlantic exchange occurs at times of reduced AMOC and NADW
290 formation, when a higher influx of IRD arrived to lower latitudes causing the freshening of Atlantic surface waters. Our results thus suggest a negative feedback between AMOC and exchange rates at the Strait of Gibraltar in the late Pliocene as it has been proposed for the late Quaternary.

Data availability. Data will be archived at PANGAEA, data publisher for Earth and Environmental Science.

295 **Competing interests.** The authors declare that they have no conflict of interest.

Acknowledgments. This project is funded by the Austrian Science Fund (FWF; project P25831-N29). We thank the Expedition 339 from the Integrated Ocean Discovery Program for providing the samples used in this study. The Bremen Core Repository is acknowledged for the sampling performed on sediment
300 cores from ODP Leg 161. Michael Joachimski from GeoZentrum Nordbayern (Erlangen) is acknowledged for performing isotopic analyses.

Figure captions

Figure 1. Location of IODP Site U1389, ODP Site 978 and the Rossello section. The map was generated
305 with GeoMapApp (<http://www.geomapapp.org>), using the default basemap, Global Multi-Resolution Topography (GMRT) Synthesis (Ryan et al., 2009).



Figure 2. (a) Stratigraphic framework established for ODP Site 978 record based on indicated biostratigraphic tie points (FO: first occurrence; LO: last occurrence) and visual correlation of the $\delta^{18}\text{O}$ record with the Rossello section (Lourens et al., 1996). **(b)** Calculated sedimentation rates.

310 **Figure 3.** $\delta^{18}\text{O}$ records of IODP Hole U1389E and ODP Site 978 from 3.33 to 2.60 Myrs. Intervals I, II and III with continuous $\delta^{18}\text{O}$ records are indicated. Marine Isotopic Stages (MIS) have been identified from Lourens et al. (1996) and Khélifi et al. (2014).

Figure 4. (a) Details of $\delta^{18}\text{O}$ records of IODP Hole U1389E and ODP Site 978 for Intervals I–III. Periods of lowered NADW and increased influx of IRD from DSDP Site 607 reported in Kleiven et al. (2002) are indicated. **(b)** Calculated $\delta^{18}\text{O}$ gradients between the Gulf of Cadiz and the Alboran Sea for glacial and interglacial stages in Intervals I–III (see Supplementary Table 2).

Figure 5. (a) Comparison of Pleistocene $\delta^{18}\text{O}$ values of *Globigerina bulloides* and *Globigerinoides ruber* at sites MD99-2336 and -2339 in the Gulf of Cadiz (Voelker et al., 2009). **(b)** Recent $\delta^{18}\text{O}$ gradients of *Gdes. ruber* between core-top samples from the Gulf of Cadiz (M39022-1; Salgueiro et al., 2008) and the Alboran Sea (stations KS82-30 and KS-82-31; Rohling, 1999). Red circles represent mean values of the respective data-sets, the red line denotes the gradient between both basins. For comparison, the gradient obtained from $\delta^{18}\text{O}$ composition of *G. bulloides* by Rogerson et al. (2010) has been added.

Supplements

325 **Supplementary Table 1.** $\delta^{18}\text{O}$ values of IODP Hole U1389E and ODP Site 978 from 3.33 to 2.60 Myrs. Intervals I, II and III are indicated.

Supplementary Table 2. Mean and standard deviation of $\delta^{18}\text{O}$ values for the studied glacial and interglacial stages of Intervals I, II and III at IODP Hole U1389E and ODP Site 978 (Fig. 3).

330

References

Ambar, I., & Howe, M.R. (1979). Observations of the Mediterranean outflow-I. Mixing the Mediterranean Outflow. Deep Sea Research 26, 535-554. doi:[https://doi.org/10.1016/0198-0149\(79\)90095-5](https://doi.org/10.1016/0198-0149(79)90095-5).



- 335 Bailey, I, Bolton, C.T., DeConto, R.M., Pollard, D., Schiebel, R., & Wilson, P.A. (2009). A low threshold for North Atlantic ice rafting from “low-slung slippery” late Pliocene ice sheets. *Paleoceanography*, 25, PA1212. doi:10.1029/2009PA001736.
- Bakun, A., Agostini, V.N. (2001). Seasonal patterns of wind-induced upwelling/downwelling in the Mediterranean Sea. *Scientia Marina* 65 (3), 243-257. doi:<http://dx.doi.org/10.3989/scimar.2001.65n3243>.
- 340 Bartoli, G., Sarnthein, M., Weinelt, & M. (2006). Late Pliocene millennial-scale climate variability in the northern North Atlantic prior to and after the onset of Northern Hemisphere glaciation. *Paleoceanography* 21, PA4205. doi:10.1029/2005PA001185.
- Bertini, A., 2010. Pliocene to Pleistocene palynoflora and vegetation in Italy: State of the art. *Quaternary International* 225, 5-24. doi:10.1016/j.quaint.2010.04.025.
- 345 Borenäs, K.M., Wåhlin, A.K., Ambar, I., & Serra, N. (2002). The Mediterranean outflow splitting—a comparison between theoretical models and CANIGO data. *Deep-Sea Research Part II: Topical Studies in Oceanography* 49, 4195–4205. doi:[https://doi.org/10.1016/S0967-0645\(02\)00150-9](https://doi.org/10.1016/S0967-0645(02)00150-9).
- Bormans, M., Garrett, C., & Thompson, R. (1986). Seasonal variability of the surface inflow through the Strait of Gibraltar. *Oceanologica Acta* 9 (4), 403–414. doi:<http://archimer.ifremer.fr/doc/00110/22092/>.
- 350 Bryden, H.L., & Kinder, T.H. (1991). Steady two-layer exchange through the Strait of Gibraltar. *Deep-Sea Research Part A. Oceanographic Research Papers* 38 (1), S445-S463. doi:[https://doi.org/10.1016/S0198-0149\(12\)80020-3](https://doi.org/10.1016/S0198-0149(12)80020-3).
- Bryden, H.L., & Stommel, H.M. (1982). Origins of the Mediterranean Outflow. *Journal of Marine Research* 40, 55–71.
- 355 Bryden, H.L., Candela, J., & Kinder, T.H. (1994). Exchange through the Strait of Gibraltar. *Progress in Oceanography* 33, 201–248.
- Budyko, M.I., Ronov, A.B., & Yanshin, A.L. (1985). *The History of the Earth’s Atmosphere*. Leningrad, Gidrometeoirdat. 209 pp. (In Russian; English translation: Springer, Berlin, 1987, 139 pp).
- 360 Cacho, I., Grimalt, J.O., Canals, M., Sbaiffi, L., Shackleton, N., Schönfeld, J., & Zahn, R. (2001). Variability of the western Mediterranean Sea surface temperature during the last 25,000 years and its connection with the northern hemisphere climatic changes. *Paleoceanography* 16, 40-52. doi:10.1029/2000PA000502.
- 365 Comas, M.C., Zahn, R., Klaus, A., et al., (1996). *Proceedings of the Ocean Drilling Program, Initial Reports*, v. 161: College Station, Texas, Ocean Drilling Program.
- DeSchepper, S., Head, M.J., & Groeneveld, J. (2009). North Atlantic Current variability through marine isotope stage M2 (circa 3.3 Ma) during the mid-Pliocene. *Paleoceanography* 24: PA4206. doi:10.1029/2008PA001725.



- 370 Dowsett, H.J., Robinson, M.M., Haywood, A.M., Hill, D.J., Dolan, A.M., Stoll, D.K., Chan, W.L., Abe-Ouchi, A., Chandler, M.A., Rosenbloom, N.A., Otto-Bliesner, B.L., Bragg, F.J., Lunt, D.J., Foley, K.M., & Riesselman, C.R. (2012). Assessing confidence in Pliocene sea surface temperatures to evaluate predictive models. *Nature Climate Change* 2, 365–371. doi:10.1038/nclimate1455.
- 375 Fauquette, S., Guiot, J., & Suc, J.-P. (1998). A method for climatic reconstruction of the Mediterranean Pliocene using pollen data. *Palaeoceanography, Palaeoclimatology, Palaeoecology* 144, 183-201. doi:[https://doi.org/10.1016/S0031-0182\(98\)00083-2](https://doi.org/10.1016/S0031-0182(98)00083-2).
- Folkard, A.M., Davies, P.A., Fiúza, A.F.G., & Ambar, I. (1997). Remotely sensed sea surface thermal patterns in the Gulf of Cadiz and the Strait of Gibraltar: Variability, correlations, and relationships with the surface wind field. *Journal of Geophysical Research* 102 (C3), 5669-5683.
- 380 García, M., Hernández-Molina, F.J., Llave, E., Stow, D.A.V., León, R., Fernández-Puga, M.C., Díaz del Río, V., & Somoza, L. (2009). Contourite erosive features caused by the Mediterranean Outflow Water in the Gulf of Cadiz: quaternary tectonic and oceanographic implications. *Marine Geology* 257, 24–40. doi:<http://dx.doi.org/10.1016/j.margeo.2008.10.009>.
- 385 García-Gallardo, Á., Grunert, P., Van der Schee, M., Sierro, F.J., Jiménez-Espejo, F.J., Álvarez-Zarikian, C.A., & Piller, W.E. (2017). Benthic foraminifera-based reconstruction of the first Mediterranean–Atlantic exchange in the early Pliocene Gulf of Cadiz. *Palaeogeography, Palaeoclimatology, Palaeoecology* 472, 93-107. doi:10.1016/j.palaeo.2017.02.009.
- Gascard, J.C., & Richez, C. (1985). Water masses and circulation in the western Alboran Sea and in the Strait of Gibraltar. *Progress in Oceanography* 15, 157-216. doi:[https://doi.org/10.1016/0079-6611\(85\)90031-X](https://doi.org/10.1016/0079-6611(85)90031-X).
- 390 Grunert, P., Balestra, B., Richter, C., Flores, J.A., Auer, G., García-Gallardo, Á., & Piller, W.E. (2017). Revised and refined age model for the upper Pliocene of IODP Site U1389 (IODP Expedition 339, Gulf of Cádiz). *Newsletters on Stratigraphy*. doi: <https://doi.org/10.1127/nos/2017/0396>.
- 395 Gudjonsson, L., & van der Zwaan, G. J. (1985). Anoxic events in the Pliocene Mediterranean: Stable isotope evidence for run-off. *Proceedings of the Koninklijke Nederlandse Akademie van Wetenschappen, Series B* 88, 69-82.
- Haywood, A.M., & Valdes, P.J. (2004). Modelling Pliocene warmth: contribution of atmosphere, oceans and cryosphere. *Earth and Planetary Science Letters* 218 (3–4), 363-377. doi:[https://doi.org/10.1016/S0012-821X\(03\)00685-X](https://doi.org/10.1016/S0012-821X(03)00685-X).
- 400 Haywood, A., Dowsett, H., Otto-Bliesner, B., Chandler, M., Dolan, A., Hill, D., Lunt, D., Robinson, M., Rosenbloom, N., Salzmann, U., & Sohl, L. (2010). Pliocene Model Intercomparison Project (PlioMIP): experimental design and boundary conditions (Experiment 1). *Geoscientific Model Development* 3 (1), 227-242. ISSN 1991-9603.
- 405 Hernández-Molina, F.J., Llave, E., Stow, D.A.V., García, M., Somoza, L., Vázquez, J.T., Lobo, F.J., Maestro, A., Díaz del Río, V., León, R., Medialdea, T., & Gardner, J. (2006). The contourite depositional system of the Gulf of Cádiz: a sedimentary model related to the bottom current activity of the Mediterranean outflow water and its interaction with the continental margin. *Deep-Sea*



- Research II Topical Studies in Oceanography 53 (11–13), 1420–1463.
doi:<http://dx.doi.org/10.1016/j.dsr2.2006.04.016>.
- 410 Hernández-Molina, F.J., Stow, D.A.V., Álvarez-Zarikian, C.A., Acton, G., Bahr, A., Balestra, B., Ducassou, E., Flood, R., Flores, J.-A., Furota, S., Grunert, P., Hodell, D., Jimenez-Espejo, F., Kim, J.K., Krissek, L., Kuroda, J., Li, B., Llave, E., Lofi, J., Lourens, L., Miller, M., Nanayama, F., Nishida, N., Richter, C., Roque, C., Pereira, H., Sanchez Goñi, M.F., Sierro, F.J., Singh, A.D., Sloss, C., Takashimizu, Y., Tzanova, A., Voelker, A., Williams, T., & Xuan, C. (2014). Onset of Mediterranean outflow into the North Atlantic. *Science* 344, 1244–1250. doi:10.1126/science.1251306.
- 415 Iorga, M.C., & Lozier, M.S. (1999). Signatures of the Mediterranean outflow from a North Atlantic climatology: 1. Salinity and density fields. *Journal of Geophysical Research* 104 (11), 259–260. doi:10.1029/1999JC900115.
- 420 Ivanovic, R.F., Valdes, P.J., Gregoire, L., Flecker, R., Gutjahr, M. (2014). Sensitivity of modern climate to the presence, strength and salinity of Mediterranean–Atlantic exchange in a global general circulation model. *Climate Dynamics* 42, 859–877. doi:10.1007/s00382-013-1680-5.
- Kaboth, S., Bahr, A., Reichart, G.-J., Jacobs, B., & Lourens, L.J. (2016). New insights into upper MOW variability over the last 150kyr from IODP 339 Site U1386 in the Gulf of Cadiz. *Marine Geology* 377, 136–145. doi:10.1016/j.margeo.2015.08.014.
- 425 Kaboth, S., Grunert, P., & Lourens, L.J. (2017). Mediterranean Outflow Water variability during the Early Pleistocene climate transition. *Climate of the Past* 13, 1023–1035. doi:<https://doi.org/10.5194/cp-13-1023-2017>.
- Khélifi, N., Sarnthein, M., Andersen, N., Blanz, T., Frank, M., Garbe-Schönberg, D., Haley, B.A., Stumpf, R., & Weinelt, M. (2009). A major and long-term Pliocene intensification of the Mediterranean outflow, 3.5–3.3 Ma ago. *Geology* 37 (9), 811–814. doi:10.1130/G30058A.1.
- 430 Khélifi, N., Sarnthein, M., Frank, M., Andersen, N., & Garbe-Schönberg, D. (2014). Late Pliocene variations of the Mediterranean outflow. *Marine Geology* 357, 182–194. doi:10.1016/j.margeo.2014.07.006.
- 435 Kleiven, H.F., Jansen, E., Fronval, T., & Smith, T.M. (2002). Intensification of Northern Hemisphere glaciations in the circum Atlantic region (3.5–2.4 Ma)—ice-rafted detritus evidence. *Palaeogeography, Palaeoclimatology, Palaeoecology* 184, 213–223. doi:[https://doi.org/10.1016/S0031-0182\(01\)00407-2](https://doi.org/10.1016/S0031-0182(01)00407-2).
- Llave, E., Hernández-Molina, F.J., Somoza, L., Stow, D.A.V., & Díaz del Río, V. (2007). Quaternary evolution of the contourite depositional system in the Gulf of Cadiz. Geological Society, London, Special publications 276, 49–79. doi:10.1144/GSL.SP.2007.276.01.03.
- 440 Lourens, L.J., Hilgen, F.J., Gudjonsson, L., & Zachariasse, W.J. (1992). Late Pliocene to early Pleistocene astronomically forced sea surface productivity and temperature variations in the Mediterranean. *Marine Micropaleontology* 19, 49–78. doi:[https://doi.org/10.1016/0377-8398\(92\)90021-B](https://doi.org/10.1016/0377-8398(92)90021-B).



- 445 Lourens, L.J., Antonarakou, A., Hilgen, F.J., Van Hoof, A.A.M., Vergnaud-Grazzini, C., & Zachariasse, W.J. (1996). Evaluation of the Plio-Pleistocene astronomical timescale. *Palaeoceanography* 11 (4), 391-413. doi:10.1029/96PA01125.
- Lunt, D.J., Haywood, A.M., Schmidt, G.A., Salzmann, U., Valdes, P.J., Dowsett, H.J., & Loptson, C.A. (2012). On the causes of mid-Pliocene warmth and polar amplification. *Earth and Planetary Science Letters* 321, 128–138. doi:<https://doi.org/10.1016/j.epsl.2011.12.042>.
- 450 Madelain, F. (1970). Influence de la topographie du fond sur l'écoulement méditerranéen entre le Déroit de Gibraltar et le Cap Saint-Vincent. *Cahiers Océanographie* 22, 43-61.
- Marchès, E., Mulder, T., Cremer, M., Bonnel, C., Hanquiez, V., Gonthier, E., & Lecroart, P. (2007). Contourite drift construction influenced by capture of Mediterranean outflow water deep-sea current by the Portimao submarine canyon (Gulf of Cadiz, south Portugal). *Marine Geology*. 242, 247–260. doi:<https://doi.org/10.1016/j.margeo.2007.03.013>.
- 455 MEDATLAS, (2002), MEDATLAS/2002 database. Mediterranean and Black Sea database of temperature salinity and biochemical parameters. Climatological Atlas: IFREMER Edition, MEDAR Group, Issy-les-Moulineaux, France.
- Millot, C. (1999). Circulation in the Western Mediterranean Sea. *Journal of Marine Systems* 20 (1-4), 423-442. doi:[https://doi.org/10.1016/S0924-7963\(98\)00078-5](https://doi.org/10.1016/S0924-7963(98)00078-5).
- 460 Millot, C. (2013). Levantine Intermediate Water characteristics: an astounding general misunderstanding! *Scientia Marina* 77 (2), 237-232. doi:10.3989/scimar.03518.13A.
- Minas, H., Coste, J.B., Le Corre, P., Minas, M., & Raimbault, P. (1991). Biological and geochemical signatures associated with the water circulation through the Straits of Gibraltar and in the western Alboran Sea. *Journal of Geophysical Research* 96 (C5), 8755-8771. doi:10.1029/91JC00360.
- 465 Ochoa, J., & Bray, N.A. (1991). Water mass exchange in the Gulf of Cadiz. *Deep Sea Research Part A. Oceanographic Research Papers*. 38:p. 465. doi:[http://dx.doi.org/10.1016/S0198-0149\(12\)80021-5](http://dx.doi.org/10.1016/S0198-0149(12)80021-5).
- 470 O'Neil, J.R., Clayton, R.N., & Mayeda, T.K. (1969). Oxygen isotope fractionation on divalent metal carbonates. *The Journal of Chemical Physics* 51, 5547–5558. doi:10.1063/1.1671982.
- Ovchinnikov, I.M. (1974). On the water balance of the Mediterranean Sea. *Oceanology* 14, 198– 202.
- Pagani, M., Liu, Z., LaRiviere, L., & Ravelo, A.C. (2010). High Earth-system climate sensitivity determined from Pliocene carbon dioxide concentrations. *Nature Geosciences* 3, 27–30. doi:10.1038/ngeo724.
- 475 Parada, M., & Cantón, M. (1998). The spatial and temporal evolution of thermal structures in the Alboran Sea Mediterranean basin. *International Journal of Remote Sensing* 19 (11), 2119– 2131. doi:<http://dx.doi.org/10.1080/014311698214901>.



- 480 Peeters, F.J.C., Brummer, G.-J.A., & Ganssen, G. (2002). The effect of upwelling on the distribution and stable isotope composition of *Globigerina bulloides* and *Globigerinoides ruber* (planktic foraminifera) in modern surface waters of the NW Arabian Sea. *Global and Planetary Change* 34, 269–291. doi:[https://doi.org/10.1016/S0921-8181\(02\)00120-0](https://doi.org/10.1016/S0921-8181(02)00120-0).
- Peliz, A., Marchesiello, P., Santos, A.M.P., Dubert, J., Teles-Machado, A., Marta-Almeida, M., Le Cann, B. (2009). Surface circulation in the Gulf of Cadiz: 2. Inflow-outflow coupling and the Gulf of Cadiz slope current. *Journal of Geophysical Research* 114, C03011. doi:[10.1029/2008JC004771](https://doi.org/10.1029/2008JC004771).
- 485 Raymo, M.E., Grant, B., Horowitz, M., & Rau, G.H. (1996). Mid-Pliocene warmth: stronger greenhouse and stronger conveyor. *Marine Micropaleontology* 27, 313–326. doi:[https://doi.org/10.1016/0377-8398\(95\)00048-8](https://doi.org/10.1016/0377-8398(95)00048-8).
- Reid, J.L. (1979). On the contribution of the Mediterranean Sea outflow to the Norwegian–Greenland Sea. *Deep-Sea Research* 26, 1199–1223. doi:[10.1016/0198-0149\(79\)90064-5](https://doi.org/10.1016/0198-0149(79)90064-5).
- 490 Rhein, M. (1995). Deep water formation in the Western Mediterranean. *Journal of Geophysical Research* 10 (C4), 6943–6959. doi:[10.1029/94JC03198](https://doi.org/10.1029/94JC03198).
- Robinson, M.M., Dowsett, H.J., & Chandler, M.A. (2008). Pliocene Role in Assessing Future Climate Impacts. *Eos* 89 (49), 501–502. doi:[10.1029/2008EO490001](https://doi.org/10.1029/2008EO490001).
- 495 Rogerson, M., Colmenero-Hidalgo, E., Levine, R.C., Rohling, E.J., Voelker, A.H.L., Bigg, G.R., Schönfeld, J., & Garrick, K. (2010). Enhanced Mediterranean–Atlantic exchange during Atlantic freshening phases. *Geochemistry, Geophysics, Geosystems* 11, Q08013. doi:[10.1029/2009GC002931](https://doi.org/10.1029/2009GC002931).
- Rogerson, M., Rohling, E.J., Bigg, G.R., & Ramirez, J. (2012). Paleooceanography of the Atlantic–Mediterranean exchange: overview and first quantitative assessment of climatic forcing. *Reviews of Geophysics* 50 (2), RG2003. doi:[10.1029/2011RG000376](https://doi.org/10.1029/2011RG000376).
- 500 Rohling, E.J. (1999). Environmental control on Mediterranean salinity and $\delta^{18}\text{O}$. *Paleoceanography* 14 (6), 706–715. doi:[10.1029/1999PA900042](https://doi.org/10.1029/1999PA900042).
- 505 Ryan, W.B.F., Carbotte, S.M., Coplan, J.O., O'Hara, S., Melkonian, A., Arko, R., Weissel, R.A., Ferrini, V., Goodwillie, A., Nitsche, F., Bonczkowski, J., & Zemsky, R. (2009). Global multi-resolution topography synthesis. *Geochemistry, Geophysics, Geosystems* 10, Q03014. doi:<http://dx.doi.org/10.1029/2008GC002332>.
- Salgueiro, E., Voelker, A.H.L., Abrantes, F., Meggers, H., Pflaumann, U., Lončarić, N., González-Álvarez, R., Oliveira, P., Bartels-Jónsdóttir, H.B., Moreno, J., & Wefer, G. (2008). Planktonic foraminifera from modern sediments reflect upwelling patterns off Iberia: Insights from a regional transfer function. *Marine Micropaleontology* 66, 135–164. doi:[10.1016/j.marmicro.2007.09.003](https://doi.org/10.1016/j.marmicro.2007.09.003).
- 510 Sarhan, T., García-Lafuente, J., Vargas, M., Vargas, J.M., & Plaza, F. (2000). Upwelling mechanisms in the northwestern Alboran Sea. *Journal of Marine Systems* 23, 317–331. doi:[https://doi.org/10.1016/S0924-7963\(99\)00068-8](https://doi.org/10.1016/S0924-7963(99)00068-8).
- Sarnthein, M., Grunert, P., Khélifi, N., Frank, M., & Nürnberg, D. (2017). Interhemispheric teleconnections: Late Pliocene change in Mediterranean outflow water linked to changes in



- 515 Indonesian Through-Flow and Atlantic Meridional Overturning Circulation, a review and update. *International Journal of Earth Sciences*. doi:<https://doi.org/10.1007/s00531-017-1505-6>.
- Seki, O., Foster, G.L., Schmidt, D.N., Mackensen, A., Kawamura, K., & Pancost, R.D. (2010). Alkenone and boron-based Pliocene pCO₂ records. *Earth and Planetary Science Letters* 292, 201–211. doi:<https://doi.org/10.1016/j.epsl.2010.01.037>.
- 520 Serra, N., Ambar, I., & Käse, R.H. (2005). Observations and numerical modeling of the Mediterranean outflow splitting and eddy generation. *Deep-Sea Research Part II: Topical Studies in Oceanography* 52, 383–408. doi:<https://doi.org/10.1016/j.dsr2.2004.05.025>.
- Shaltout, M., & Omstedt, A. (2014). Recent sea surface temperature trends and future scenarios for the Mediterranean Sea. *Oceanologia* 56 (3), 411–443. doi:<https://doi.org/10.5697/oc.56-3.411>.
- 525 Stow, D.A.V., Hernández-Molina, F.J., & Alvarez-Zarikian, C. (2013). Expedition 339 summary. *Proceedings of the Integrated Ocean Drilling Program*. doi:<http://dx.doi.org/10.2204/iodp.proc.339.104.2013>.
- Thunell, R.C., & Williams, D.F. (1989). Glacial-Holocene changes in the Mediterranean Sea: hydrographic and depositional effects. *Nature* 338, 493–496.
- 530 Tzanova, A., & Herbert, T. (2015). Regional and global significance of Pliocene sea surface temperatures from the Gulf of Cadiz (Site U1387) and the Mediterranean. *Global and Planetary Change* 133, 371–377. doi:<http://dx.doi.org/10.1016/j.gloplacha.2015.07.001>.
- Van der Schee, M., Sierro, F.J., Jiménez-Espejo, F.J., Hernández-Molina, F.J., Flecker, R., Flores, J.A., Acton, G., Gutjahr, M., Grunert, P., García-Gallardo, Á., & Andersen, N. (2016). Evidence of early bottom water current flow after the Messinian Salinity Crisis in the Gulf of Cadiz. *Marine Geology* 380, 315–329. doi:<http://dx.doi.org/10.1016/j.margeo.2016.04.005>.
- 535 Van Os, B.J.H., Lourens, L.J., Hilgen, F.J., & De Lange, G.J. (1994). The Formation of Pliocene sapropels and carbonate cycles in the Mediterranean: Diagenesis, dilution, and productivity. *Paleoceanography* 9 (4), 601–617. doi:10.1029/94PA00597.
- 540 Vargas-Yáñez, M., Plaza, F., García-Lafuente, J., Sarhan, T., Vargas, J.M., & Vélez-Belchi, P. (2002). About the seasonal variability of the Alboran Sea circulation. *Journal of Marine Systems* 35, 229–248. doi:[https://doi.org/10.1016/S0924-7963\(02\)00128-8](https://doi.org/10.1016/S0924-7963(02)00128-8).
- Vergnaud-Grazzini, C., Ryan, W.B.F., & Cita, M.B. (1977). Stable isotope fractionation, climatic change and episodic stagnation in the eastern Mediterranean during the late Quaternary. *Marine Micropaleontology* 2, 353–370. doi:[https://doi.org/10.1016/0377-8398\(77\)90017-2](https://doi.org/10.1016/0377-8398(77)90017-2).
- 545 Voelker, A.H.L., Lebreiro, S.M., Schönfeld, J., Cacho, I., Erlenkeuser, H., & Abrantes, F. (2006). Mediterranean outflow strengthening during northern hemisphere coolings: A salt source for the glacial Atlantic? *Earth and Planetary Science Letters* 245, 39–55. doi:<https://doi.org/10.1016/j.epsl.2006.03.014>.



- 550 Voelker, A.H.L., Schönfeld, J., Erlenkeuser, H., & Abrantes, F. (2009). Hydrographic conditions along the western Iberian margin during marine isotope stage 2. *Geochemistry, Geophysics, Geosystems* 10 (12), Q12U08. doi:10.1029/2009GC002605.
- Voelker, A.H.L., Salgueiro, E., Rodrigues, T., Jimenez-Espejo, F.J., Bahr, A., Alberto, A., Loureiro, I., Padilha, M., Rebotim, A., & Röhl, U. (2015). Mediterranean outflow and surface water variability off southern Portugal during the early Pleistocene: a snapshot at marine isotope stages 29 to 34 (1020–1135 ka). *Global and Planetary Change* 133, 223–237. doi:10.1016/j.gloplacha.2015.08.015.
- 555
- Wüst, G. (1961). On the vertical circulation of the Mediterranean Sea. *Journal of Geophysical Research* 66, 3261–3271. doi:10.1029/JZ066i010p03261.
- 560 Zenk, W. (1975). On the Mediterranean outflow west of Gibraltar. *Meteor-Forschungsergebnisse A* (16), 23–34.



Table 1. Maximum, minimum, mean and standard deviation of $\delta^{18}\text{O}$ values of IODP Hole U1389E and ODP Site 978 in the long term and within Intervals I, II, and III.

565

Period	Long term (3.33-2.60 Myrs)		Short terms					
			Interval I (2.73-2.60 Myrs)		Interval II (3.02-2.88 Myrs)		Interval III (3.33-3.27 Myrs)	
Site ID	Hole U1389E	Site 978	Hole U1389E	Site 978	Hole U1389E	Site 978	Hole U1389E	Site 978
Min	-1.22	-1.81	-1.22	-1.34	-0.99	-1.64	-0.85	-1.11
Max	0.98	0.68	0.46	0.49	0.98	0.5	0.7	0.54
Average	-0.14	-0.41	-0.34	-0.39	-0.16	-0.5	-0.05	-0.2
SD	0.37	0.51	0.38	0.52	0.39	0.54	0.31	0.44



Figure 1

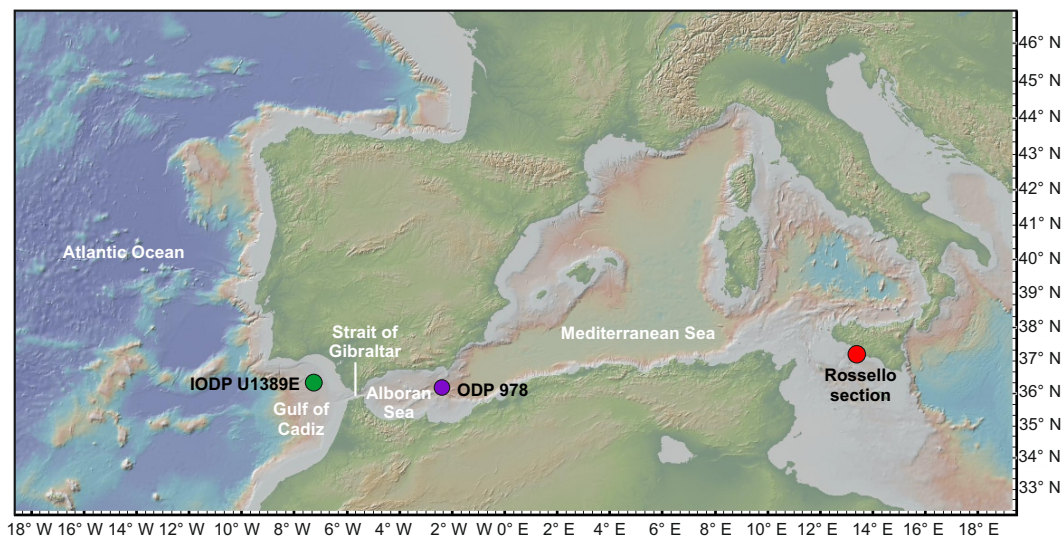




Figure 2

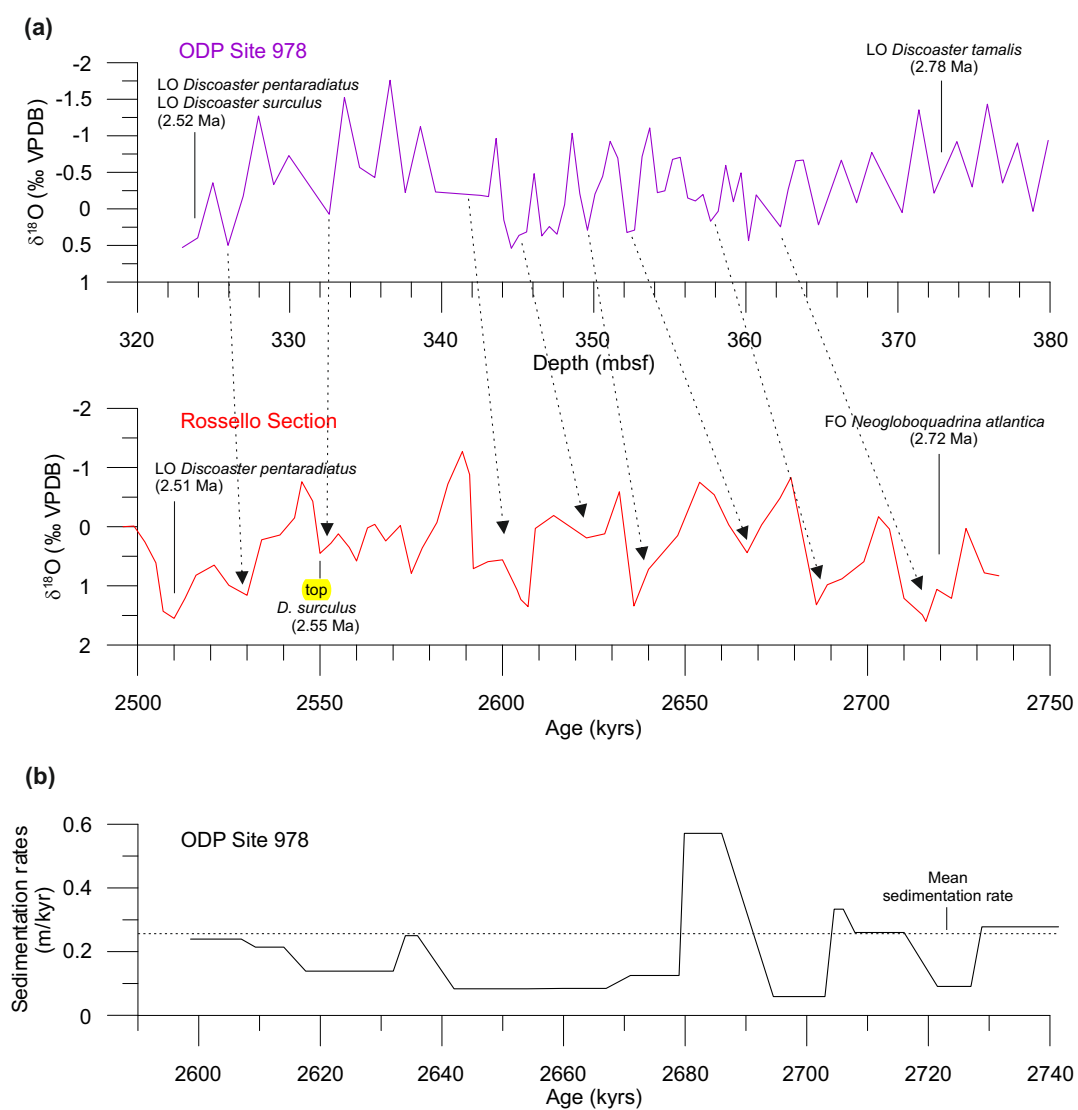




Figure 3

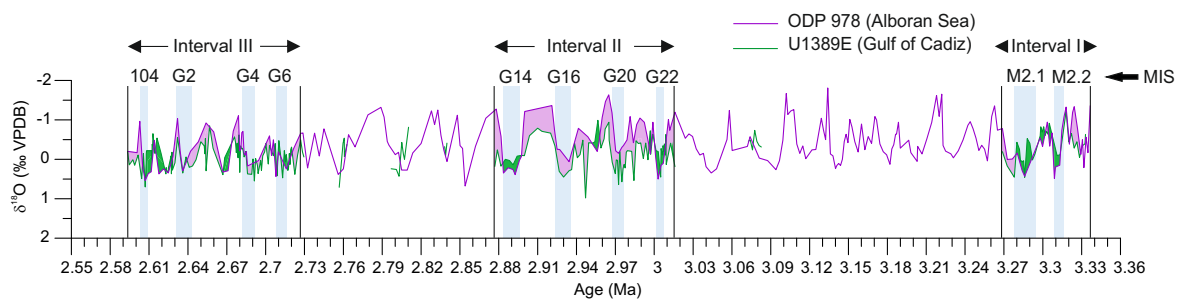




Figure 4

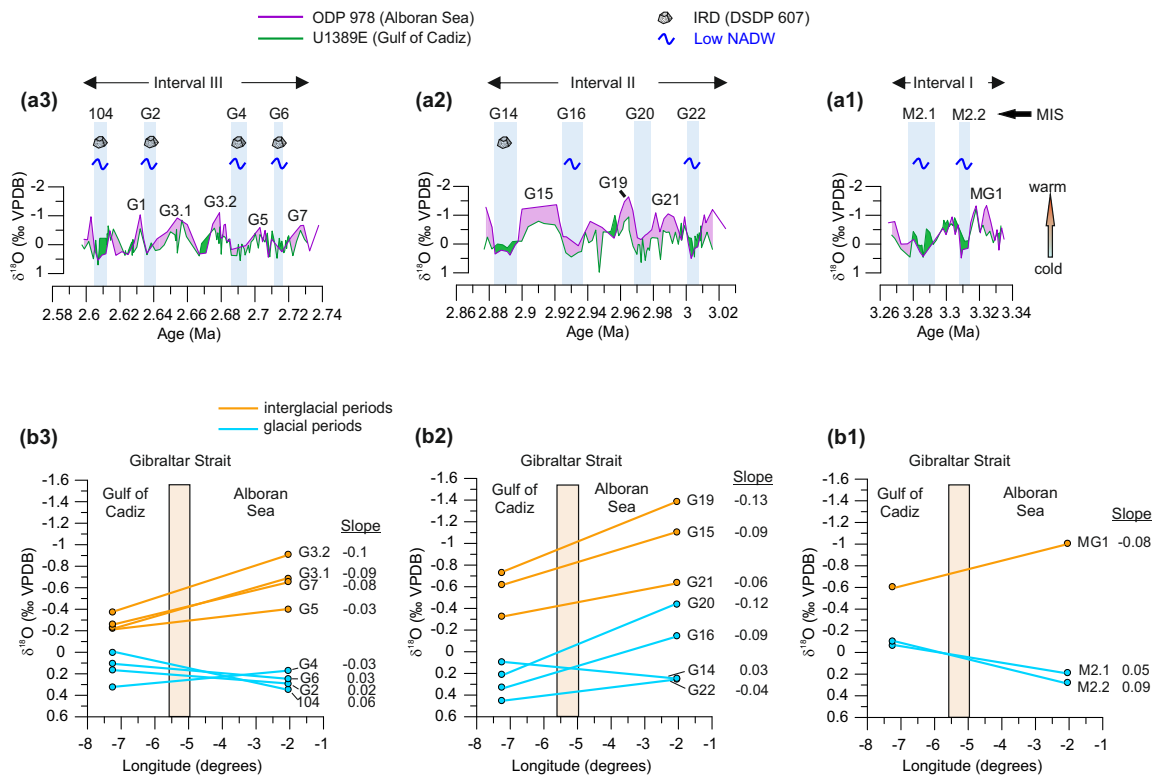




Figure 5

